ELSEVIER

Journal of Nuclear Materials 258–263 (1998) 289–294

journal of nuclear materials

Calculation of radiation-induced deformation in the ITER vacuum vessel

Johsei Nagakawa *

National Research Institute for Metals, 1-2-1 Sengen, Tsukuba, Ibaraki 305-0047, Japan

Abstract

Numerical calculation was carried out to evaluate the radiation induced deformation at the blanket side of the vacuum vessel (120°C) and the rear portion of the blanket module (200°C) in ITER. The calculation was performed for solution-annealed 316 stainless steel mainly at 1×10^{-9} dpa/s and 100 MPa. Enhanced transient creep characteristic of the low temperature irradiation is evident at 120°C. However, the total accumulated creep strain in the vacuum vessel is only below 0.01% for the lifetime irradiation so that serious consequence would not be anticipated. At the rear portion of the blanket the creep strain would be about 0.01% and not serious either. Radiation-induced stress relaxation at the vacuum vessel is only several per cent during the lifetime. At the rear portion of the blanket, on the other hand, the relaxation could be of the order of 10% and should not be completely neglected.

1. Introduction

Very significant irradiation creep strain, larger than at 300–400°C, has been observed for both austenitic and ferritic stainless steels in the ORNL/ORR in-reactor experiments at 60°C and about 7 dpa [1]. Considerable creep enhancement has also been observed recently in the 17 MeV proton in-beam experiments of 316 stainless steel at 60°C [2]. The present author has reported the results of a numerical calculation which directly simulated the early stage of irradiation creep at 60 and 300°C for 316 stainless steel [3]. The calculation revealed that the significant deformation enhancement during the 60°C irradiation results from the overwhelming interstitial flux during the transient period of the point defect kinetics.

These experimental and calculational results suggest that the radiation-induced deformation could be of importance to the design assessments of some of the ITER (International Thermonuclear Experimental Reactor) components subject to the irradiation at temperatures lower than that of the first wall. For instance, 316 stainless steel of the blanket side of the vacuum vessel will be irradiated at a displacement rate of 10^{-9} dpa/s or so at about 120°C (cooled with water of 100°C at the inlet and 111°C at the outlet). The rear portion of the blanket module, also made of 316 stainless steel, is expected to be irradiated at a similar displacement rate around 200°C or lower (cooled with water of 140°C at the inlet and 191°C at the outlet). However, the database of radiation-induced deformation at these lower temperatures and very low displacement rates is not complete, even for such a widely used nuclear material as 316 stainless steel. Moreover, extrapolation would be inappropriate since the defect kinetics is still in the transient stage and the deformation is not a simple linear function of accumulated damage and its rate.

In this paper, the simulation calculation is applied to evaluate the two aspects of radiation-induced deformation, irradiation creep and radiation-induced stress relaxation, of solution annealed 316 stainless steel at the portions of ITER, particularly the vacuum vessel, where irradiation at lower temperatures and lower displacement rates is expected. Although the total accumulated damage during the lifetime at such portions should be very low, i.e., only 0.1 dpa or so, the very low displacement rate and the possible transient nature would

* Tel.: +81-298 59 2014/2839; fax: +81-298 59 2014; e-mail: johsei@nrim.go.jp.

0022-3115/98/$19.00 © 1998 Elsevier Science B.V. All rights reserved.
PII: S 0 0 2 2 - 3 1 1 5 (9 8) 0 0 0 8 7 - 7

make the experimental evaluation very difficult and the calculational evaluation essential.

2. Modeling and calculation procedure

The calculation is based on the stress-influenced kinetics of nucleation and growth of defect agglomerates, as well as point defect absorption by network dislocations. Simultaneous differential equations are numerically solved for the following defect concentrations: (1) single interstitials (C_i), (2) single vacancies (C_v), (3) aligned interstitial loop precursors (C_{2iA}), (4) non-aligned interstitial loop precursors (C_{2iN}), (5) growing interstitial loops on aligned planes (C_{ilA}), (6) those on non-aligned planes (C_{ilN}), (7) accumulated net interstitials in growing aligned loops (C_{ilAi}), (8) those in growing non-aligned loops (C_{ilNi}), (9) net interstitials absorbed by aligned network dislocations (C_{dAi}), (10) those absorbed by non-aligned network dislocations (C_{dNi}).

In the calculation, the point defect migration energies for the 316 stainless steel were taken from the evaluation by Dimitrov and Dimitrov [4], that is, 0.92 eV for interstitials and 1.15 eV for vacancies, which has been substantiated by the studies on microstructure evolution [5]. Important parameter values used in the numerical calculation are listed in Table 1. Z_i (interstitial bias) and ΔZ_i (stress-induced bias) for loops and network dislocations were calculated using the equations given by Wolfer [6] and Heald [7], respectively. At each numerical iteration step, the loop size was re-averaged and $Z_{i,v}$ and $\Delta Z_{i,v}$ were re-evaluated. In the interstitial loop nucleation process, di-interstitial was provided to be the precursor and its formation was considered to be affected by the external stress following the SIPN model proposed by Brailsford and Bullough [8].

In the present study, SIPN (Stress-Induced Preferential Nucleation of interstitial loops) [8,9] and loop growth driven by SIPA (Stress-Induced Preferred Absorption of point defects) [7,10] are taken into account, as well as PA (SIPA climb) and PAG (glide enabled by SIPA climb) contributions [11] by network dislocations. From the calculated derivatives of defect concentrations, plastic strain rate produced by each mechanism was evaluated at every iteration step using the following equations;

(1) PA (SIPA climb creep by network dislocations) [11]

$$\dot{\varepsilon}_{PA} = \frac{2}{3}(\mathrm{d}C_{dAi}/\mathrm{d}t - \mathrm{d}C_{dNi}/\mathrm{d}t). \tag{1}$$

(2) PAG (dislocation glide induced by SIPA climb) [11]

$$\dot{\varepsilon}_{PAG} = (4e\sqrt{(\pi L_d)}/3b)(\mathrm{d}C_{dAi}/\mathrm{d}t - \mathrm{d}C_{dNi}/\mathrm{d}t). \tag{2}$$

(3) SAIL (SIPA climb creep by growing interstitial loops) [7,10]

$$\dot{\varepsilon}_{SAIL} = \frac{2}{3}(\mathrm{d}C_{ilAi}/\mathrm{d}t - \mathrm{d}C_{ilNi}/\mathrm{d}t). \tag{3}$$

(4) SIPN (creep by stress-induced preferential loop nucleation) [8,9]

$$\dot{\varepsilon}_{SIPN} = \frac{4}{3}(\mathrm{d}C_{2iA}/\mathrm{d}t - \mathrm{d}C_{2iN}/\mathrm{d}t), \tag{4}$$

Table 1
Parameter values used in the calculation

Parameter	Value
Defect migration energy	
Interstitial	0.92 eV
Vacancy	1.15 eV
Defect migration pre-exponent	
Interstitial	8.0×10^{-7} m^2/s
Vacancy	1.4×10^{-6} m^2/s
Lattice constant	3.524×10^{-10} m
Atomic volume	1.1×10^{-29} m^3
Strength of Burgers vector	2.1×10^{-10} Mpa
Young's modulus	2.6×10^5 Mpa
Shear modulus	1.0×10^5 Mpa
Poisson's ratio	0.3
Dislocation density	3×10^{12} m/m^3
Defect relaxation volume (*in atomic volume*)	
Interstitial	$+1.4 \times$ atomic volume
Vacancy	$-0.46 \times$ atomic volume
Deference in shear modulus between defect and matrix	
Interstitial	-1.0×10^5 Mpa
Vacancy	0 Mpa

where e is the elastic deflection (σ/E; σ is the external stress, E is Young's modulus), L_d is the network dislocation density, and b is the size of the Burgers vector. The damage efficiency used for the neutron irradiation was 0.3. This value was selected because the in-reactor creep compliance is generally about 0.3 times that for the light-ion irradiation creep [12]. For the latter case, the efficiency is usually regarded as close to unity and the calculation with the efficiency of 1 showed a very good coincidence with the experimental data including temperature dependence [3]. In the following, a nominal dpa, not the value multiplied by the damage efficiency, is used to describe the damage and the damage rate unless otherwise indicated. The calculation was performed mainly at 120°C and 200°C, i.e., the expected temperature of the vacuum vessel and the rear portion of the blanket, respectively, with some references at 60°C and 300°C.

3. Results and discussion

3.1. Irradiation creep deformation

Fig. 1 shows the calculated creep strain rate as a function of time at 1×10^{-9} dpa/s and 100 Mpa. Creep rates at 60°C and 300°C are also shown for reference. Even at 300°C initial transient period appears at a very early stage of irradiation (up to about 3×10^3 s), but it diminishes swiftly without contributing noticeable strain and a steady creep rate follows. In contrast, at 60°C the transient region is prolonged to a great extent (about 5×10^{10} s), resulting in a moderate strain production. At 120°C the behavior is just in-between. The transient lasts up to about 1×10^8 s (0.1 dpa) but beyond that a steady creep rate appears. At 200°C the behavior is closer to that of the 300°C irradiation. The transient is only up to about 4×10^5 s (4×10^{-4} dpa) and does not contribute much to the creep strain. These points can be visualized more easily in Fig. 2 where accumulated irradiation creep strain is plotted for the dpa range of 0.001–1 dpa. The enhanced irradiation creep at 60°C induces more strain than at the higher temperature of 300°C in the earlier stage, but its falling creep rate allows the latter to overwhelm it in the higher dpa region. When the displacement rate is much higher than 1×10^{-9} dpa/s, the predominance of the low temperature irradiation creep persists to much higher damage [3]. More detailed discussion of the difference in the irradiation creep behavior between low and high temperatures will be given in a separate paper [13]. At 120°C, the typical temperature of the vacuum vessel, the irradiation creep shifts from the

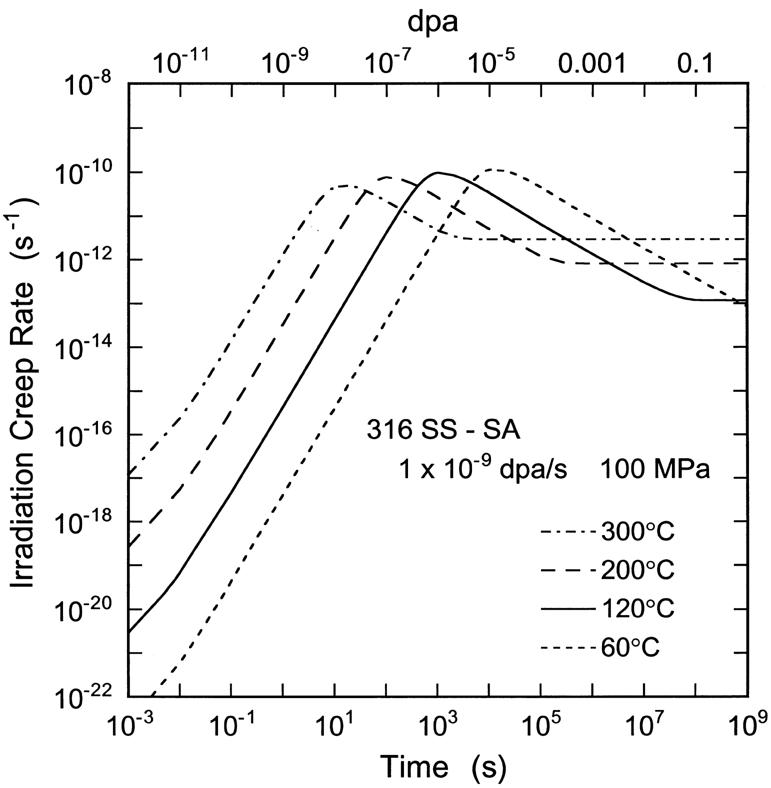

Fig. 1. Irradiation creep rate vs. time for solution-annealed 316SS at 1×10^{-9} dpa/s and 100 MPa.

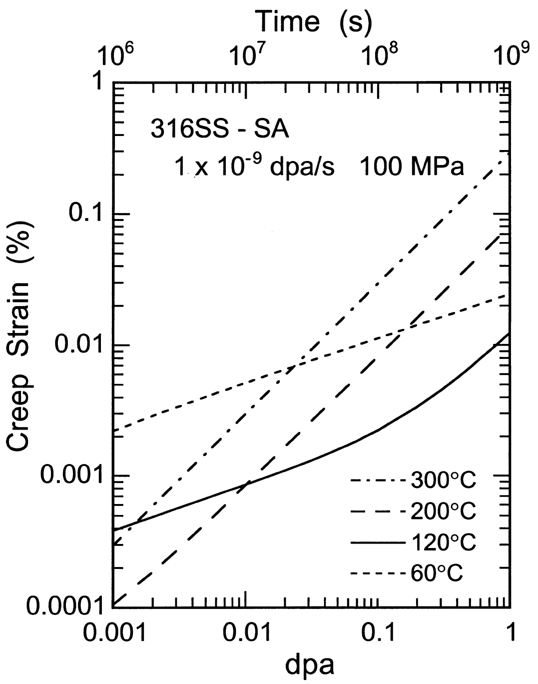

Fig. 2. Irradiation creep strain vs. dpa for solution-annealed 316SS at 1×10^{-9} dpa/s and 100 MPa.

low temperature type to the high temperature once the damage is accumulated. The total creep strain produced up to 0.1 dpa is only about 0.002%. At 200°C the irradiation creep behavior is similar to the 300°C case except for the very low damage region. The total creep strain at 200°C is still below 0.01% at 0.1 dpa. Therefore, the accumulated irradiation creep strain would remain at most or below 0.01% during the lifetime in both the vacuum vessel and the rear portion of the blanket module under the external applied stress of 100 MPa. In both cases the amount of irradiation creep strain is quite small and does not appear to be detrimental for the rather low stresses expected especially at the vacuum vessel.

3.2. Radiation-induced stress relaxation

Since the most steels have an elastic modulus of around 2×10^5 MPa from room temperature to 500°C, only a minute plastic strain of 0.05% is enough to completely relax the initial stress of 100 MPa. This very small strain is yet quite difficult to produce in the unirradiated condition but not so under irradiation. When the creep rate is constant and expressed in a form of the power law, the stress relaxation can be obtained analytically even for the irradiation case [14]. However, such analytical evaluation would not be appropriate if the creep is still in transient and its rate changes continuously. In the following, stress relaxation is calculated directly by the computer simulation. The amount of stress reduction $\Delta\sigma$ by the total plastic strain $\Delta\varepsilon_p$ produced by all the four mechanisms during each iteration step was evaluated using the equation

$$\frac{d\sigma}{dt} = -E\frac{d\varepsilon_p}{dt} \Rightarrow \Delta\sigma = -E\,\Delta\varepsilon_p. \tag{5}$$

All kinetic parameters for the next iteration step were recalculated with the newly evaluated stress value [14].

Figs. 3 and 4 show the stress relaxation curves up to 1 dpa at the irradiation temperature of 120°C and

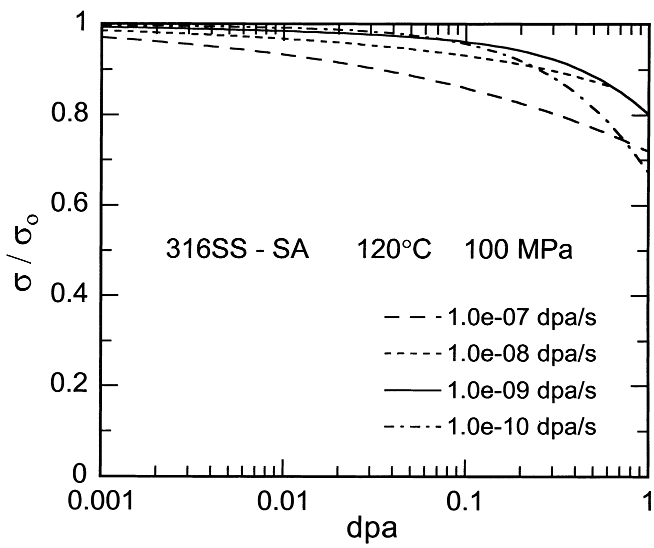

Fig. 3. Radiation-induced stress relaxation of solution-annealed 316SS at 120°C and 1×10^{-9} dpa/s with the initial stress of 100 MPa.

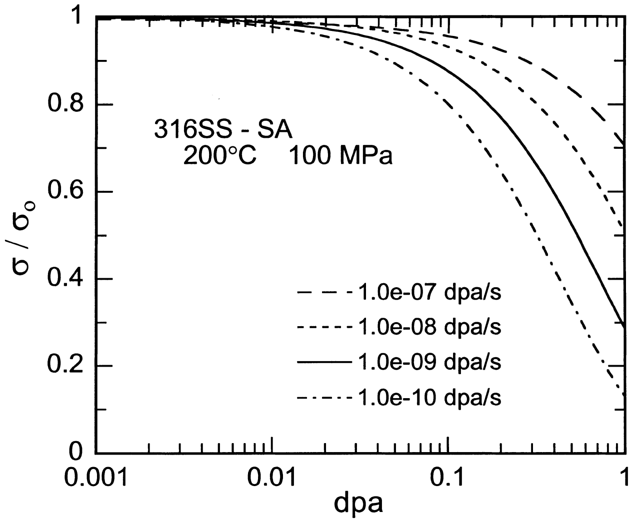

Fig. 4. Radiation-induced stress relaxation in solution-annealed 316SS at 200°C and 1×10^{-9} dpa/s with the initial stress of 100 MPa.

200°C, respectively, for the range of displacement rates from 10^{-7} to 10^{-10} dpa/s. Although the difference in temperature is only 80°C between the two cases, the difference in the stress relaxation curve is rather conspicuous. At 120°C the stress relaxation does not differ so much among the range of displacement rates, it is only a little larger at the highest rate. At 200°C the relaxation is more enhanced as the displacement rate decreases. At 120°C such a negative dependence can also be noticed for 10^{-9} and 10^{-10} dpa/s, while the dependence is positive for 10^{-7} and 10^{-8} dpa/s. More extensive calculation for the low displacement rates [13] indicated that the enhanced deformation due to the transient kinetics at low temperatures causes larger relaxation with higher displacement rate. This is associated with higher interstitial flux to sinks, leaving vacancies in the matrix, when the displacement rate is higher. At higher temperatures, where the transient completes at a very early stage, the deformation rate is negatively dependent on the displacement rate when the sink density is low and the recombination is one of the major processes of defect annihilation as in the present condition. Fig. 5 shows the initial stress dependence of the stress relaxation ratio at 0.01, 0.1 and 1 dpa for 120°C. A slight dependence on the initial stress can be noticed. This may correspond to the stress dependence of the transient irradiation creep

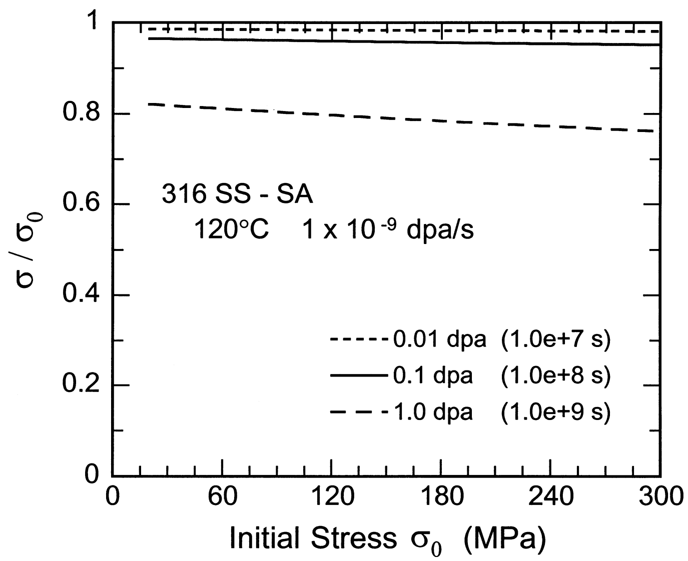

Fig. 5. Initial stress dependence of the relaxation in solution-annealed 316 SS at 120°C and 1×10^{-9} dpa/s.

rate at low temperatures, which is slightly stronger than linear relationship [15]. However, the stress dependence is so weak that even a very small stress is expected to be relaxed at a similar rate as the much larger stresses.

From Figs. 3 and 5 it could be concluded that the radiation induced stress relaxation at the blanket side of the vacuum vessel is only several per cent during its lifetime irradiation (0.1 dpa or so) and does not appear to be very detrimental. At the rear portion of the blanket, on the other hand, the relaxation would be of the order of 10% as shown in Fig. 4 and should not be completely neglected in some cases. More extensive calculation [13] indicates that the stress relaxation at the same low displacement rates becomes much more enhanced when the irradiation temperature is decreased to 60°C or increased to 300°C. Therefore, the temperature range of 120–200°C happens to be a better choice in view of the radiation-induced stress relaxation.

4. Conclusion

Numerical computer calculation was carried out to assess the radiation induced deformation at the blanket side of the vacuum vessel and the rear portion of the blanket module in ITER. The calculation was performed for solution annealed 316 stainless steel mainly at 120 and 200°C, 1×10^{-9} dpa/s and 100 MPa. The results can be summarized as follows.

1. Enhanced transient irradiation creep characteristic of the low temperature irradiation is evident at 120°C. However, the total accumulated creep strain in the vacuum vessel (120°C) is only below 0.01% for the lifetime irradiation so that serious consequence would not be expected. At the rear portion of the blanket (200°C) the creep strain would be about 0.01% and not serious either.
2. Radiation-induced stress relaxation at the vacuum vessel is only several per cent during the lifetime. At the rear portion of the blanket, on the other hand, the relaxation could be of the order of 10% and should not be completely neglected.

References

[1] M.L. Grossbeck, L.K. Mansur, J. Nucl. Mater. 179 (1991) 130.
[2] Y. Murase, J. Nagakawa, N. Yamamoto, to be submitted.
[3] J. Nagakawa, N. Yamamoto, H. Shiraishi, J. Nucl. Mater. 179 (1991) 986.
[4] C. Dimitrov, O. Dimitrov, J. Phys. F 14 (1984) 793.
[5] N. Yoshida, J. Nucl. Mater. 205 (1993) 344.
[6] W.G. Wolfer, M. Ashkin, J. Appl. Phys. 46 (1975) 547; 46 (1975) 4108.
[7] P.T. Heald, M.V. Speight, Philos. Mag. 29 (1974) 1075.
[8] A.D. Brailsford, R. Bullough, Philos. Mag. 27 (1973) 49.
[9] R.V. Hesketh, Philos. Mag. 7 (1962) 1417.
[10] R. Bullough, J.R. Willis, Philos. Mag. 31 (1975) 855.
[11] L.K. Mansur, Philos. Mag. A 39 (1979) 497.
[12] P. Jung, J. Nucl. Mater. 113 (1983) 133.
[13] J. Nagakawa, to be submitted.
[14] J. Nagakawa, J. Nucl. Mater. 212 (1994) 541.
[15] J. Nagakawa, J. Nucl. Mater. 225 (1995) 1.